The Particle Collection Efficiency Curves by the Porous Substrate of an Inertial Impactor

Cheng-Hsiung Huang[1]*, Chuen-Jinn Tsai[2]

[1] *Department of Environmental Engineering and Health, Yuanpei Institute of Science and Technology, No. 306 Yuanpei St., 300 Hsinchu, Taiwan, ROC*
[2] *Institute of Environmental Engineering, National Chiao Tung University, No. 75 Poai St., 300 Hsinchu, Taiwan, ROC*

This work numerically studied particle collection efficiency curves as a function of aerodynamic particle diameter by the porous substrate of an inertial impactor. The simulation was conducted for different Reynolds numbers based on nozzle diameter (Re), resistance factors of porous substrate (K) and nozzle diameters of the inertial impactor (W). The results show that average flow velocity inside the porous substrate is low for a particle starting from the position close to the centerline leading to a small inertial force. The collection efficiency curves of the inertial impactor with porous substrate are less sharp for the case of higher Re and lower K than the case of lower Re and higher K. This phenomenon occurs because more air penetrates into the porous substrate when Re is large and K is small, resulting in higher particle collection efficiency. The cutoff aerodynamic diameter, d_{p50}, of the impactor with porous substrate decreases with increasing Re, decreasing K and decreasing W. Ultrafine particle loss in the porous substrate can be important. For example, the particle loss of a three-stage cascade inertial impactor with porous substrate increases to 16.5 % for particles with an aerodynamic diameter of 0.01 μm due to the diffusion mechanism when K = 568,000 cm^{-2} and Q = 2 L/min.

Keywords: Collection efficiency curve, inertial impactor, porous substrate

1. Introduction

Inertial impactors are widely used for measuring the particle size distribution and chemical composition of aerosols. The performance of a well-designed impactor has a sharp particle collection efficiency curve following the traditional theory (Marple 1970; Marple and Liu 1974; Marple and Willeke 1976; Rader and Marple 1985). A common problem of inertial impactors with flat platesubstrate is particle bounce-off and reentrainment, which can cause bias in particle size distribution measurement (Rao and Whitby 1978; Biswas and Flagan 1988; Pak et al. 1992; Xu and Willeke 1993). An alternative to conventional substrate impactors, polyurethane foam (PUF) was used effectively as the substrate for conventional inertial impators (Kavouras and Koutrakis 2001). Experimental results showed that PUF substrates absorbed more excess kinetic energy than did conventional flat plate substrates, reducing the amount of particles that would otherwise bounce off or be reentrained.

Additionally, porous metal substrate was also used as the collection surface of an inertial

*Corresponding author:
Tel.: +886-3-5381183 ext. 8354
Fax: +886-3-5381183 ext. 8353
E-mail address: chhuang@pc.ymit.edu.tw

impactor (Tsai et al. 2001). Experimental results showed that the inertial impactor with the porous metal substrate had the advantage of allowing the sampling of a high concentration of liquid particles without overloading because of its capillary action. The particle collection efficiency of the impactor with the porous metal substrate was higher than that with the flat plate substrate, due to air penetration into the porous metal substrate resulting in a different particle collection efficiency curve (Huang et al. 2001) than predicted by the traditional theory. The ultrafine particles will be collected on the upper stages of the inertial impactor with the porous substrates resulting in the bias of particle size distribution measurement.

In this study, to investigate the particle collection efficiency curves as a function of aerodynamic particle diameter by the porous substrate of the inertial impactor, flow field and particle trajectories of the inertial impactor were simulated. The filtration efficiency of particles inside the porous substrate was calculated at different resistance factors of the porous substrate, nozzle diameters and Reynolds numbers. Subsequently, the particle collection efficiency curves were obtained under different situations for aerodynamic particle diameters ranging from 0.001 to 10 μm.

2. Numerical Method

The flow field in the inertial impactor was simulated by solving the 2-D Navier-Stokes equations in the cylindrical coordinate (Huang et al. 2001). The fluid flow in the impactor was assumed steady, incompressible and laminar, and air was assumed to be at 20 °C and 1 atm. The governing equation was discretized by means of the finite volume method and solved by the SIMPLE algorithm (Patankar 1980). The flow field is governed by

$$\rho\left(\vec{V}\bullet\vec{\nabla}\right)\vec{V} = -\vec{\nabla}P + \mu\nabla^2\vec{V} - K\mu\vec{V} \qquad (1)$$

In equation (1) $\vec{V}$ is velocity vector in cm/s; P the pressure in dyne/cm^2; ρ the air density in g/cm^3; μ the air viscosity in g/cm-s; K the resistance factor of the porous substrate in cm^{-2} (K = 1/k , k is the permeability). After obtaining the flow field, the particle equations of the motion were solved numerically to obtained particle trajectories and collection efficiency. The particle equations of motion in r (radial) and z (axial) directions are:

$$m_p\frac{du_{pr}}{dt} = C_d\,Re_p\frac{\pi\mu d_p}{8C}\left(u_r - u_{pr}\right) \qquad (2)$$

$$m_p\frac{du_{pz}}{dt} = C_d\,Re_p\frac{\pi\mu d_p}{8C}\left(u_z - u_{pz}\right) + m_p g \qquad (3)$$

In the above equations, C_d is the empirical drag coefficient; Re_p the particle Reynolds number; m_p and g the particle mass and the gravitational acceleration, respectively; u_{pr} and u_{pz} the particle velocities; u_r and u_z local flow velocities in the radial and axial directions, respectively.

The particle collection efficiency of the impactor with porous substrate can be defined as the collection efficiency, based on the ideal (or 100 %) filtration efficiency, multiplied by the average filtration efficiency by the porous substrate and can be calculated as

$$\eta = \eta_{f100\%} \times \eta_{Tave} \qquad (4)$$

where $\eta_{f100\%}$ and η_{Tave} are the 100 % filtration efficiency and the average filtration efficiency by the porous substrate and can be calculated as

$$\eta_{f100\%} = \left[Rc/(W/2)\right]^2 \qquad (5)$$

$$\eta_{Tave} = \sum_{i=1}^{Rc} Q_i \times \eta_{Tmi} / Q_c \qquad (6)$$

where W is the nozzle diameter and Rc is the critical radius across the nozzle which demarcates the starting radial position for a particle to be collected by the substrate or not. If a particle starts at a radial position smaller than Rc, then the particle will be collected. It can be calculated by a

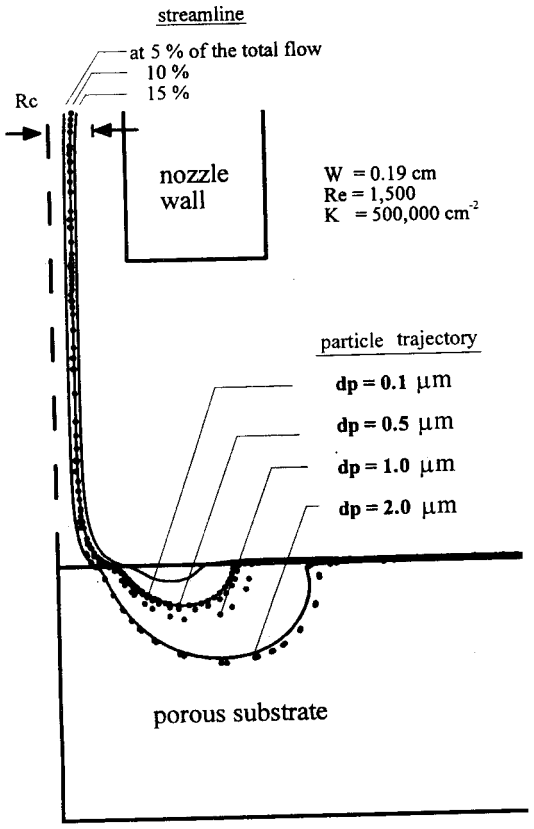

Fig. 1. Particle trajectories for the particle starting at the radial position of particles released in the nozzle corresponding to 10 % of the total flow and streamlines at 5 %, 10 % and 15 % of the total flow.

numerical method based on the assumption that particle concentration and velocity profiles are uniform at the entrance of the nozzle. Q_i denotes the flow rate represented by the i-th radial position at the inlet of the nozzle, Q_c is the flow rate corresponding to the critical radius and η_{Tmi} is the average filtration efficiency of η_{Ti} for a particle entering at i-th radial position. η_{Ti} can be expressed by Flagan and Seinfeld (1988) as

$$\eta_{Ti} = 1 - \exp\left[-4\alpha\eta_F L/\pi(1-\alpha)d_f\right] \tag{7}$$

where $\eta_F = \eta_D + \eta_G + \eta_R + \eta_I$ is the collection efficiency of a single-collector including diffusion, gravity, interception and impaction, α is the solid volume fraction and L is the distance. The effective collector diameter of porous substrate, d_f, can be approximated by

$$d_f = \left[16\alpha(1+2\upsilon)/\chi K R_h\right]^{1/2} \tag{8}$$

where χ, υ, and R_h is the inhomogeneity factor, slip coefficient and hydrodynamic factor, respectively.

Since the porous substrate has a granular-like structure consisting of powder sintered together, the prediction equations of Otani et al. (1989) based on experimental data in a wide range of filtration condition were used to calculate the collection efficiency of individual mechanism. The single-collection efficiency due to diffusion can be calculated as

$$\eta_D = A Sc^B Re_f^C \tag{9}$$

$$\begin{cases} B = -\dfrac{2}{3} + \dfrac{Re_f^3}{6\left(Re_f^3 + 2.0\times 10^5\right)} \\ A = 8.0,\ C = -2/3, \text{ for } Re_f < 30 \\ A = 40.0,\ C = -1.15, \text{ for } 30 \le Re_f < 100 \\ A = 2.1,\ C = -1/2, \text{ for } Re_f \ge 100 \end{cases} \tag{10}$$

where the parameter Sc = Pe / Re_f, Pe and Re_f are the Peclet and Reynolds number which are defined as

$$Pe = u_0 d_f / D \tag{11}$$

$$Re_f = \rho u_0 d_f / \mu \tag{12}$$

where D is the diffusion coefficient; u_0 the average air velocity inside porous substrate.

The single-collection efficiency by gravity can be calculated as

$$\eta_G = G/(1+G) \tag{13}$$

(a)

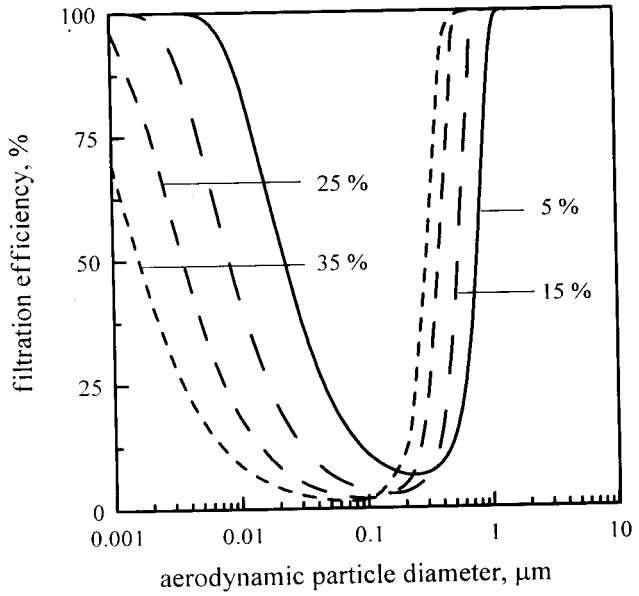

Fig. 2. (a) Filtration efficiency curves of the impactor with the porous substrate at different radial positions of particles released in the nozzle corresponding to 5, 15, 25 and 35 % of the total flow. K = 500,000 cm^{-2} and Re = 3,000

(b)

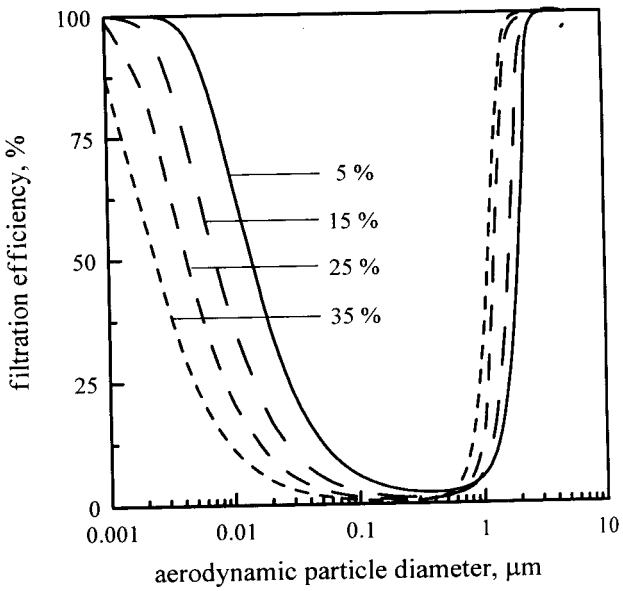

Fig. 2. (b) Filtration efficiency curves of the impactor with the porous substrate at different radial positions of particles released in the nozzle corresponding to 5, 15, 25 and 35 % of the total flow. K = 100,000 cm^{-2} and Re = 1,000.

where the parameter G is defined as

$$G = Cd_p^2 g(\rho_p - \rho)/18\mu u_0 \quad (14)$$

The single-collection efficiency by interception can be calculated as

$$\eta_R = 16R^{2-Re_f/(Re_f^{1/3}+1)^3} \quad (15)$$

where the parameter $R = d_p/d_f$.

The single-collection efficiency by impaction can be calculated as

$$\eta_I = St_{eff}^3/(0.014 + St_{eff}^3) \quad (16)$$

where St_{eff} is defined as

$$St_{eff} = St_f[Re_f(1-\alpha)/86\alpha + 1] \quad (17)$$

where St_f is defined as

$$St_f = \rho_p d_p^2 u_0 C/9\mu d_f \quad (18)$$

3. Results and Discussion

3.1 Particle Trajectories

Fig. 1 illustrates the particle trajectories for the different particle diameters starting at the radial position of particles released in the nozzle corresponding to 10 % of the total flow and streamlines at 5 %, 10 % and 15 % of the total flow at K = 500,000 cm^{-2}, W = 0.19 cm and Re = 1,500. The boundary conditions of the nozzle wall and the back of the substrate were considered as solid boundary. The figure shows that the streamlines in the porous substrate curve up because of theresistant force from the substrate. In addition, for the case of the streamline position close to the centerline of the nozzle, the penetrating air has the longer distance inside the porous substrate and the lower flow velocities caused by the resistance of the substrate. Thus, the average flow velocity is

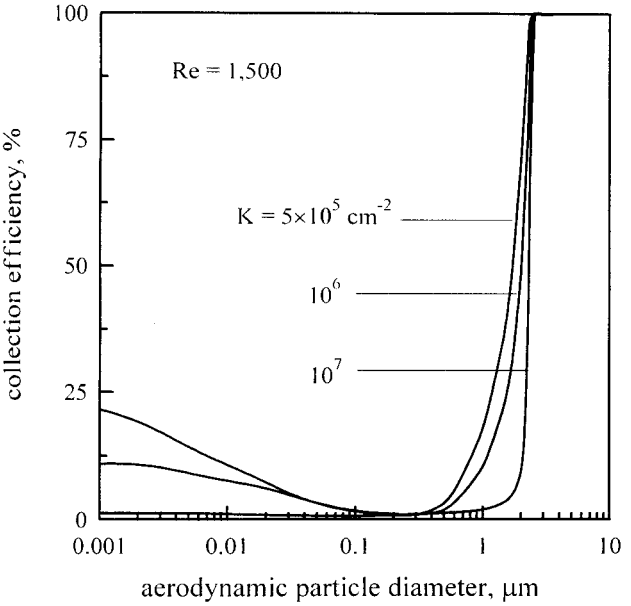

Fig. 3. Effect of Re on the particle collection efficiency curve by the porous substrate of the impactor, K = 568,000 cm^{-2} and W = 0.19 cm.

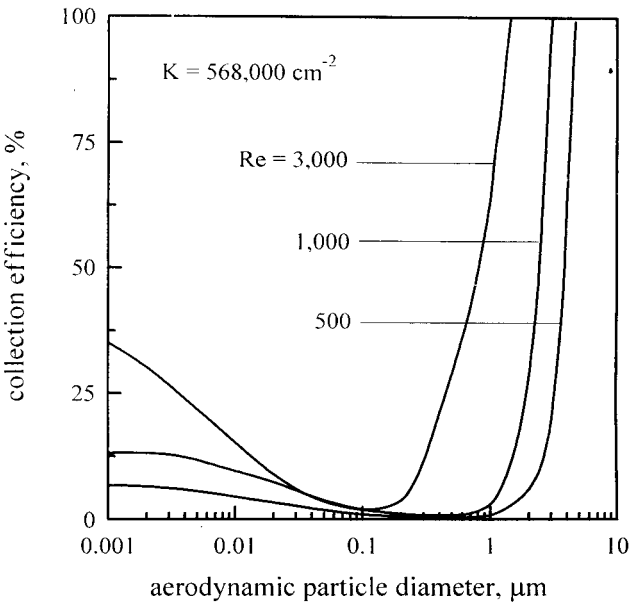

Fig. 4. Effect of K on the particle collection efficiency curve by the porous substrate of the impactor, Re = 1,500 and W = 0.19 cm.

low for the streamline position close to the centerline inside the porous substrate. The particle trajectories of the small particles, i.e. d_p = 0.1 and 0.5 μm, are close to the air streamlines. For particles with large particle diameters, i.e. d_p = 1.0 and 2.0 μm, the particle trajectories deviate from the corresponding streamlines due to their high inertial force. The particles will be collected inside the porous substrate as the result of the filtration mechanism including the inertial impaction, diffusion, interception, and gravitational settling.

3.2 Filtration Efficiency Curves

The particles released from different locations of the nozzle have different filtration efficiency curves by the porous substrate. Fig. 2 shows the filtration efficiency curves of the impactor with porous substrate at different radial positions of particles released in the nozzle for K = 500,000 cm^{-2} and Re = 3,000 (Fig. 2a) and K = 100,000 cm^{-2} and Re =1,000 (Fig 2b). In both cases, it is seen that there is a substantial shift of filtration efficiency curves to the left for the position farther away from the centerline in comparison with the position closer to the centerline. It is because that the average flow velocity inside the porous substrate is low for a particle starting from the position close to the centerline leading to a small inertial force. There are minimum filtration efficiencies of about 0.5 ~ 10 % at the particle diameters of 0.05 ~ 0.3 μm in the curves. When the particle diameters are small, the filtration efficiency increases with decreasing particle diameter due to the particle diffusion. For large particles, the filtration efficiency increases with an increase in the particle diameter due to the interception and impaction.

3.3 Effect of Reynolds Number

Fig. 3 shows the particle collection efficiency curves by porous substrate of the impactor at three different Reynolds numbers for the resistance factor of 568,000 cm^{-2} and the nozzle diameter of 0.19 cm. It is seen that the curve becomes less sharp as Re is increased and the collection efficiency curve is more S-shaped like for Re = 3,000. The cutoff

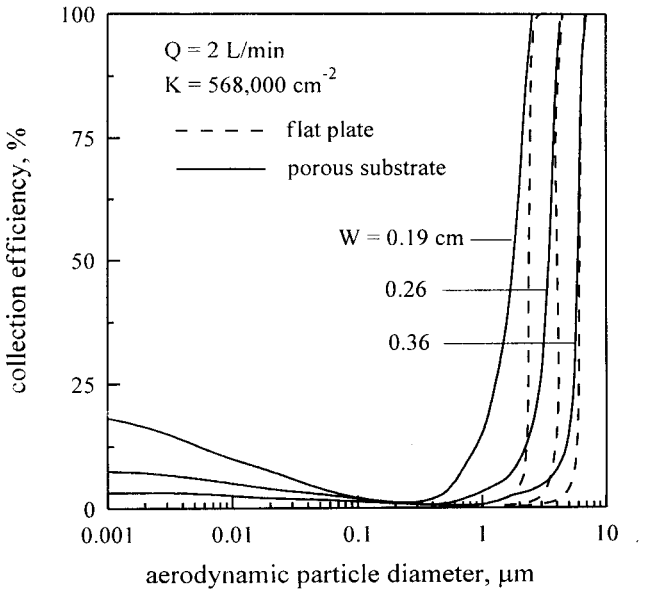

Fig. 5. Particle collection efficiency curve by the porous substrate of the impactor at different W, K = 568,000 cm^{-2} and Q = 2 L/min.

aerodynamic diameter, d_{p50}, of the impactor with porous substrate decreases with an increasing Re and is found to be 3.83, 2.42 and 0.81 μm for Re = 500, 1,000 and 3,000, respectively. There is a minimum collection efficiency value of about 1.9, 0.8 and 0.3 % at d_p = 0.1, 0.3 and 0.5 μm for Re = 3,000, 1,000 and 500, which corresponds to the most difficult particle diameter to collect during the impaction process. For ultrafine particle with d_p = 0.01 μm, the collection efficiency increases to 15.2, 9.6 and 4.5 % for Re = 3,000, 1,000 and 500, respectively. When Re is larger, the airflow penetrates into the porous substrate more easily resulting in higher particle collection efficiency due to diffusion mechanism.

3.4 Effect of Resistance Factor

Fig. 4 shows the particle collection efficiency curves by porous substrate of the impactor at three different resistance factors for Re = 1,500 and the nozzle diameter of 0.19 cm. It is seen that the d_{p50} of the impactor with porous substrate increases with an increasing K and it is found to be 1.72, 2.02 and 2.31 μm for K = 5×10^5, 10^6 and 10^7 cm^{-2}, respectively. This is because that more air penetrates into the porous substrate resulting in higher coarse particle collection efficiency due to inertial impaction mechanism when K is smaller. There is a minimum collection efficiency value of about 0.9, 0.9 and 0.7 % at d_p = 0.3, 0.3 and 0.1 μm and the collection efficiency of the particle of d_p = 0.01 μm is found to be 10.7, 7.5 and 1.0 % for K = 5×10^5, 10^6 and 10^7 cm^{-2}, respectively. As K is large as 10^7 cm^{-2}, the ultrafine particle collection efficiency can be neglected because the airflow is difficult to penetrate into the porous substrate.

3.5 Particle Collection Efficiency Curves at Different Nozzle Diameters

Fig. 5 shows the particle collection efficiency curves by porous substrate of the impactor for three different nozzle diameters at K = 568,000 cm^{-2} and Q = 2 L/min. It is seen that there is a shift of the collection efficiency curve of the impactor with the porous substrate (solid lines) to the left of the flat plate impactor (dotted lines), and the deviation in the curves increases with a decreasing W. The d_{p50} of the impactor with porous substrate is found to be 1.79, 3.47 and 5.94 μm, and that of flat plate impactor is 2.40, 3.81 and 6.15 μm for W = 0.19, 0.26 and 0.36 cm, respectively. The minimum collection efficiency is about 1.2, 0.8 and 0.5 % at d_p = 0.3, 0.5 and 0.5 μm for W = 0.19, 0.26 and 0.36 cm, respectively. The ultrafine particle loss for d_p of 0.01 μm in the porous substrate due to diffusion mechanism is found to be 9.9, 5.0 and 2.5 % for W = 0.19, 0.26 and 0.36 cm, respectively. In this case, the ultrafine particle loss is calculated to be 16.5 % for a three-stage cascade inertial impactor at a flow rate of 2 L/min. This loss is not negligible when designing an inertial impactor with porous substrates.

4. Conclusions

The collection efficiency of ultrafine particles must be considered when designing an inertial impactor with porous substrate because ultrafine particles collected on the upper stages create a bias in particle size distribution measurement. Besides the bias caused by ultrafine particles, the d_{p50} of the inertial impactor with porous substrate is also critical to particle size distribution analysis. This study shows that a leftwards shift occurs in filtration efficiency curves for positions further away from the centerline compared to those closer to the centerline. This phenomenon occurs because the average flow velocity inside the porous substrate is low for particles starting close to the centerline, leading to a small inertial force. The d_{p50} of the inertial impactor with porous substrate is smaller than that of the flat plate impactor and deviation in the collection efficiency curves increases with decreasing nozzle diameter. When Re is high and K is low, the d_{p50} of the impactor is smaller due to more effective inertial impaction near the surface. The minimum collection efficiency is about 0.3 ~ 1.9 % for particle diameters of 0.1 ~ 0.5 μm, Re ranging from 500 to 3,000 and K ranging from 5×10^5 to 10^7 cm^{-2}. In case that K = 568,000 cm^{-2} and Q = 2 L/min, particle loss of a 0.01 μm particle in aerodynamic diameter in a three-stage cascade impactor with porous substrate is estimated to be as high as 16.5 % due to diffusion mechanism.

Acknowledgments

The authors would like to thank the National Science Council of the Republic of China, Taiwan for financially supporting this project under Contract No. NSC 90-2218-E-264-005.

References

Biswas P. and Flagan R. C. (1988), The Particle Trap Impactor. J. Aerosol Sci. 19: 113-121.

Flagan R. C. and Seinfeld J. H. (1988), Fundamentals of Air Pollution Engineering, Englewood Cliffs, New Jersey.

Huang C. H., Tsai C. J. and Shih T. S. (2001), Particle Collection Efficiency of an Inertial Impactor with Porous Metal Substrates. J. Aerosol Sci. 32: 1035-1044.

Kavouras I. G. and Koutrakis P. (2001), Use of Polyurethane Foam as the Impaction Substrate/Collection Medium in Conventional Inertial Impactors. Aerosol Sci. Technol. 34: 46-56.

Marple V. A. (1970), A Fundamental Study of Inertial Impactors. Ph. D. thesis, University of Minnesota, Minneapolis, MN.

Marple V. A. and Liu B. Y. H. (1974), Characteristics of Laminar Jet Impactors. Environ. Sci. Technol. 8: 648-654.

Marple V. A. and Willeke K. (1976), Impactor Design. Atmos. Environ. 10: 891-896.

Otani Y., Kanaoka C. and Emi H. (1989), Experimental Study of Aerosol Filtration by the Granular Bed over a Wide Range of Reynolds Numbers. Aerosol Sci. Technol. 10: 463-474.

Pak S. S., Liu B. Y. H. and Rubow K. L. (1992), Effect of Coating Thickness on Particle Bounce in Inertial Impactors. Aerosol Sci. Technol. 16: 141-150.

Patankar S. V. (1980), Numerical Heat Transfer and Fluid Flow, Hemisphere, Washington, DC.

Rader D. J. and Marple V. A. (1985), Effect of Ultra-Stokesian Drag and Particle Interception on Impaction Characteristics. Aerosol Sci. Technol. 4: 141-156.

Rao A. K. and Whitby K. T. (1978), Non-Ideal Collection Characteristics of Inertial Impactors-I: Single-Stage Impactors and Solid Particles. J. Aerosol Sci. 9: 77-86.

Tsai C. J., Huang C. H., Wang S. H. and Shih, T. S. (2001), Design and Testing of a Personal Porous-Metal Denuder. Aerosol Sci. Technol. 35: 611-616.

Xu M. and Willeke K. (1993), Right Angle Impaction and Rebound of Particles. J. Aerosol Sci. 24: 19-30.

Received for review, February 18, 2002
Accepted, April 17, 2002
AAQR-2002-01